CMS Physics Analysis Summary

Contact: cms-pag-conveners-susy@cern.ch 2011/08/24

Search for Supersymmetry in Events with Photons, Jets and Missing Energy

The CMS Collaboration

Abstract

This PAS describes two searches for supersymmetry in a gauge-mediation scenario, with the gravitino as the lightest supersymmetric particle. The data sample corresponds to an integrated luminosity of 1.14 fb^{-1} recorded by the CMS experiment at the LHC. We compare the missing transverse energy distribution in events containing either at least two photons and at least one hadronic jet, or exactly one photon and at least three jets, to the spectra expected from standard model processes. No excess of events at high missing transverse energy is observed and upper limits on the signal cross section between 0.015 and 0.2 pb at the 95% confidence level are determined for a range of squark, gluino, and neutralino masses.

Supersymmetry (SUSY), in particular the version based on gauge-mediated SUSY breaking[1–7], is of high theoretical interest for physics beyond the standard model (SM). It stabilizes the mass of the SM Higgs boson, drives the grand unification of forces, and avoids the flavor problems endemic in other SUSY breaking scenarios. Previous searches for SUSY with gauge-mediated breaking were performed at ATLAS [8], CMS [9], as well as the Tevatron [10, 11], LEP [12–15], and HERA [16]. The CMS search was mostly sensitive to colored SUSY particle production, and, using a simplified model [17], constrained their masses to be above 500 GeV/c^2. The other searches put constraints on the gauge boson partners, with the current best lower limit on the neutralino mass [11] of 175 GeV/c^2 in a general gauge-mediation (GGM) SUSY scenario similar to what is studied here.

In this paper we consider a GGM scenario [18, 19], with the gravitino ($\tilde{G}$) as the lightest SUSY particle (LSP) and the lightest neutralino ($\tilde{\chi}_1^0$) as the next-to-lightest SUSY particle (NLSP). Long-lived neutralino scenarios are not covered in this analysis. The gravitino escapes detection, leading to missing transverse energy (E_T^{miss}) in the event. Assuming that R-parity [20] is conserved, strongly-interacting SUSY particles are pair-produced at the LHC. Their decay chain includes one or several quarks/gluons, and a neutralino, which in turn decays to a gravitino and a photon or a Z boson.

We also investigate the scenario where the NLSP is a pure wino. In that case, the lightest chargino ($\tilde{\chi}_1^{\pm}$) is also a wino, and the chargino-neutralino mass difference is too small for one to decay into the other. In that case the chargino will decay directly into a gravitino and a W boson.

The two topologies studied in this search are:

- two (or more) isolated photons with transverse energy E_T above 45 and 30 GeV, at least one hadronic jet, and large E_T^{miss};
- exactly one isolated photon with E_T above 75 GeV, at least three hadronic jets, and large E_T^{miss}.

In neither topology do we veto on additional leptons, as especially in the wino co-NLSP case doing so would significantly restrict acceptance of the neutralino decays into Z and chargino decays into $W\pm$ which could be present for higher neutralino masses. Table 1 gives example decay chains leading to these final states. The table is divided horizontally between single-photon vs diphoton target final states. The vertical direction differentiates between bino NLSP and wino co-NLSP cases. The number of jets produced in the cascades can vary depending on whether gluinos or squarks are produced and the species of quarks in the final state. (for example one can imagine with a high enough gluino mass decaying into pairs of $t\bar{t}$ which might generate as many as half a dozen jets.)

Table 1: Some general characteristics of the GGM cascades leading to the topologies of interest

NLSP type	γ + 3 jets + E_T^{miss}	$\gamma\gamma$ + jet + E_T^{miss}
Bino	jets + $\tilde{\chi}_1^0\tilde{\chi}_1^0 \rightarrow$ jets + $\gamma + Z + \tilde{G}\tilde{G}$	jets + $\tilde{\chi}_1^0\tilde{\chi}_1^0 \rightarrow$ jets + $\gamma\gamma + \tilde{G}\tilde{G}$
Wino	jets + $\tilde{\chi}_1^0\tilde{\chi}_1^0 \rightarrow$ jets + $\gamma + Z + \tilde{G}\tilde{G}$ jets + $\tilde{\chi}_1^0\tilde{\chi}_1^{\pm} \rightarrow$ jets + $\gamma + W^{\pm} + \tilde{G}\tilde{G}$	jets + $\tilde{\chi}_1^0\tilde{\chi}_1^0 \rightarrow$ jets + $\gamma\gamma + \tilde{G}\tilde{G}$

A detailed description of the CMS detector can be found elsewhere [21]. The detector's central feature is a superconducting solenoid providing a 3.8 T axial magnetic field along the beam direction. Charged particle trajectories are measured by a silicon pixel and strip tracker

system, covering $0 \leq \phi \leq 2\pi$ in azimuth and $|\eta| < 2.5$, where the pseudorapidity $\eta = -\ln[\tan\theta/2]$, and θ is the polar angle with respect to the counterclockwise beam direction. A lead-tungstate crystal electromagnetic calorimeter (ECAL) and a brass/scintillator hadron calorimeter (HCAL) surround the tracker volume. For the barrel calorimeter ($|\eta| < 1.479$), the modules are arranged in projective towers. Muons are measured in gas detectors embedded in the steel return yoke of the magnet. The detector is nearly hermetic, allowing for reliable measurement of $E_{\mathrm{T}}^{\mathrm{miss}}$. In the 2011 collision data, photons with energy greater than 30 GeV are measured within the barrel ECAL with a resolution of better than 1% [22], which is dominated by inter-calibration precision.

The data used in this analysis were recorded during the current 2011 LHC run using the CMS two-level trigger system, based on the presence of at least one high-energy photon and significant hadronic activity or at least two photons, and corresponds to an integrated luminosity of 1.14 fb^{-1}. This data sample is utilized for the selection of both signal candidates and control samples used for background estimation. The efficiency for signal events satisfying off-line selection to pass the trigger is estimated to be above 99% for both analyses. The particular triggers used for the single-photon and diphoton analyses are discussed below.

The photon candidates are reconstructed from clusters of energy in the ECAL. Candidate events are required to have exactly one (at least two) photon(s) with a minimum transverse energy for the single-photon (diphoton) analysis. We require the ECAL cluster shape to be consistent with that expected from a photon, and the ratio of the energy detected in HCAL behind the photon shower not to exceed 5% of the ECAL energy. To suppress hadronic jets giving rise to photon candidates, we require the latter to be isolated from other activity in the tracker, ECAL and HCAL. A cone of $\Delta R = \sqrt{(\Delta\eta)^2 + (\Delta\phi)^2} = 0.4$ is constructed around the candidates' direction, and the scalar sums of transverse energies of tracks and calorimeter deposits within this ΔR are determined, after excluding the contribution from the candidate itself. The isolation sums are required to be $< 0.001 \times E_{\mathrm{T}} + 2.0$ GeV, $< 0.006 \times E_{\mathrm{T}} + 4.2$ GeV, and $< 0.0025 \times E_{\mathrm{T}} + 2.2$ GeV, for the tracker, ECAL and HCAL, respectively.

Photons that fail either the shower shape or track isolation requirement are referred to as *fake photons*. These objects are dominantly electromagnetically fluctuated jets and are used for the background estimation from data.

The criteria above are efficient for the selection of both electrons and photons. To reliably separate them, we search for hit patterns in the pixel detector consistent with a track from an electron (pixel match). The candidates without pixel match are considered to be photons. Otherwise they are considered to be electrons, which we will use to select control samples for background estimation.

Jets and $E_{\mathrm{T}}^{\mathrm{miss}}$ are reconstructed with a particle-flow technique [23]. This algorithm reconstructs all particles produced in the collision and subsequently identifies them as charged or neutral hadrons, photons, muons, and electrons, by combining information from all detector subsystems. All these particles are clustered into jets using the anti-K_T clustering algorithm with distance parameter of 0.5. To be counted, a jet must have transverse momentum $p_{\mathrm{T}} \geq 30$ GeV/c, $|\eta| \leq 2.6$ and is required to satisfy jet ID requirements, namely: The fraction of energy contributed to the shower by the highest energy hadronic calorimeter element be $\leq 99\%$, that no single HCAL channel contain more than 90% of the jet energy, and that the jet's electromagnetic fraction be $\geq 1\%$. The events must contain at least one such jet isolated from the photon candidates by $\Delta R \geq 0.5$ for the events to be retained in the signal sample.

The SUSY signal of interest can be mimicked by SM processes in several ways. Irreducible

backgrounds from SM processes such as $Z(\rightarrow \nu\bar{\nu})\gamma\gamma$ and $W(\rightarrow \ell\nu)\gamma\gamma$ are negligible. The main backgrounds arise from standard model processes with misidentified photons and/or mismeasured $E_{\mathrm{T}}^{\mathrm{miss}}$. The dominant contribution comes from the mis-measurement of $E_{\mathrm{T}}^{\mathrm{miss}}$ in QCD processes such as direct diphoton, photon plus jets, and multijet production, with jets mimicking photons. This background is referred to as *QCD background*. The strategy for determining this background is to use control samples which are kinematically similar to the candidate sample while having no true $E_{\mathrm{T}}^{\mathrm{miss}}$.

The second background comes from events with true $E_{\mathrm{T}}^{\mathrm{miss}}$. It is dominated by events with a real or fake photon and a W boson that decays into a neutrino and an electron, which is misidentified as a photon. We refer to this sample as the *Electroweak background* (EWK). Since all components of this background involve electron-photon misidentification, in order to estimate its contribution to the signal sample, we weight a sample of $e\gamma$ events with $f_{e\rightarrow\gamma}/(1-f_{e\rightarrow\gamma})$ where $f_{e\rightarrow\gamma}$ is the probability to misidentify an electron as a photon. This $e\gamma$ sample has the same requirements imposed on it as the candidate $\gamma\gamma$ sample except a pixel seed is required for one of the EM objects. We also use a sample of ee events where pixel seeds are required on both objects. We measure $f_{e\rightarrow\gamma} = 0.014 \pm 0.0004\,(\mathrm{stat.}) \pm 0.002\,(\mathrm{syst.})$ by determining the number of $Z \rightarrow ee$ events in the ee and $e\gamma$ samples.

To study certain SM processes and to generate SUSY signal events, we use the PYTHIA[24] event generator. In particular, we generate SUSY GGM events in a three-dimensional grid of the NLSP, gluino, and squark masses in the benchmark model [17]. Squarks are taken to be mass-degenerate. All other SUSY particles are assumed to be heavy. The production cross-section at NLO QCD is calculated for these points using PROSPINO [25], and is dominated by gluino-gluino, gluino-squark, and squark-squark production. The generated events are then passed through the CMS detector simulation program [26] and reconstructed using the same program as for the collision data so that all features of the detector are included in the signal Monte Carlo acceptances.

In the following we first describe the results of the diphoton analysis and then summarize the search for GGM SUSY production using single-photon events. The diphoton analysis is based on a diphoton trigger with a threshold ranging from 32 GeV (22 GeV) to 40 GeV (28 GeV) for the leading (sub-leading) photon over the course of the data taking period. To be in a range of flat trigger efficiency, the offline analysis requires at least two photons with $E_{\mathrm{T}} > 45$ GeV (30 GeV) for the the leading (sub-leading) photon in the event.

To estimate the QCD background from data, we utilize two different data sets. The first sample contains two fake photons, in what follows referred to as the fake-fake (ff), comprising QCD multijet events. The second sample contains events with two electrons (ee) with the invariant mass between 70 and 110 GeV/c^2, and is dominated by $Z \rightarrow ee$ decays. The E_{T} resolution for electrons and fake photons is similar to the resolution for true photons, and is negligible compared with the resolution for hadronic energy, resulting in the $E_{\mathrm{T}}^{\mathrm{miss}}$ resolution to be dominated by the latter. The events in both control samples are re-weighted to reproduce the photon(s) transverse energy distribution in the data, and, therefore, the transverse energy of hadronic recoil against the photon(s). The $E_{\mathrm{T}}^{\mathrm{miss}}$ distributions in the re-weighted control samples are identical within the uncertainties, and their shape is used to determine the magnitude of the QCD background. The QCD predictions from the ff and ee samples are found to agree after all cuts are applied in both a nominal signal region of $E_{\mathrm{T}}^{\mathrm{miss}} > 100$ GeV and a loose region of $E_{\mathrm{T}}^{\mathrm{miss}} > 50$ GeV. The estimates are combined to form an error weighted average QCD prediction. In the E_{T} region of 30 to 50 GeV we observe 127 candidate diphoton events, while our combined background estimate in this same region predicts $125.1 \pm 5.1\,(\mathrm{stat.}) \pm 41.4\,(\mathrm{syst.})$. The

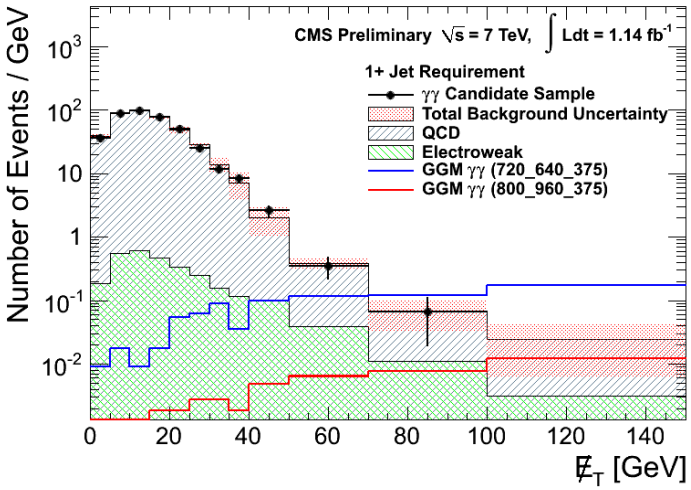

Figure 1: E_T^{miss} spectrum of $\gamma\gamma$ data compared to combined QCD prediction together with the small EWK background for events with ≥ 1 jet. The red hatched areas indicate the total background uncertainties. Two example GGM points on either side of our exclusion boundary ($m_{\tilde{q}}$_m_{sGlu}_$m_{\tilde{\chi}_1^0}$ in GeV/c^2) are also shown.

estimated EWK background is determined with ee and $e\gamma$ samples as described above and is calculated to be much smaller than the QCD background. Other backgrounds have been found to be negligible.

The E_T^{miss} distribution in the $\gamma\gamma$ sample requiring ≥ 1 jet is represented in Fig. 1 as points with errors bars. The green hatched area shows the estimated amount of the EWK background. We assume that events with $E_T^{miss} \leq 20$ GeV have negligible SUSY signal contribution, and scale the E_T^{miss} distributions of the average QCD prediction so that the integral of the distribution below 20 GeV matches that in the $\gamma\gamma$ sample minus the estimated EWK contribution. The red hatched areas indicate the total background uncertainties.

We perform an optimization of the search region in E_T^{miss} that is expected to give the best limit possible for the production of GGM SUSY processes. This procedure results in a cut on $E_T^{miss} \geq 100$ GeV. Table 2 summarizes the observed number of $\gamma\gamma$ events with $E_T^{miss} \geq 100$ GeV and the expected backgrounds with the statistical uncertainty and errors due to re-weighting and normalization shown separately. We observe zero events while the background expectation is calculated to be 2.5 ± 2.2 (1.3 ± 0.8) events using the ff (ee) samples. Table 3 provides observed event yields and background estimates for a "loose signal region" corresponding to the 50 GeV E_T^{miss} requirement of reference [9]. In this case we observe 9 events with an estimated background of 11.3 ± 1.9 (stat.) ± 0.8 (syst.).

We determine the efficiency for SUSY events to pass our analysis cuts by applying correction factors derived from the data to the MC simulation of the signal. Since there is no large clean sample of photons in the data, we rely on similarities between the detector response to electrons and photons to extract the photon efficiency. We obtain a scale factor to apply to the photon MC efficiencies by making a ratio of electron efficiency from $Z \rightarrow ee$ events that pass all photon ID cuts (except for the pixel match in data) and the corresponding electron MC efficiencies. We apply the obtained scale factor 0.953 ± 0.014 (stat.) ± 0.068 (syst.) to the MC photon efficiencies calculated with MC simulation. Other sources of the larger systematic uncertainties in the signal yield include the error on integrated luminosity (4.5%), pile-up effects (2.5%), PDF un-

Table 2: The number of events with $E_{\mathrm{T}}^{\mathrm{miss}} \geq 100$ GeV from $\gamma\gamma$, ff, and $Z \to ee$ as well as the total number of background events with $E_{\mathrm{T}}^{\mathrm{miss}} \geq 100$ GeV using either the ff events or the $Z \to ee$ data. We also show the contributions to the errors from statistics, the error due to the scaling technique and normalization.

Type	Events	stat. error	scal. error	norm. error
$\gamma\gamma$ candidates	0			
ff QCD background	2.3 ± 2.2	± 2.19	± 0.13	± 0.10
ee QCD background	1.0 ± 0.8	± 0.82	± 0.02	± 0.03
EWK background	0.3 ± 0.1	± 0.06	± 0.0	± 0.03
Total background (ff)	2.5 ± 2.2			
Total background (ee)	1.3 ± 0.8			

Table 3: The number of events in the "loose signal" region of $E_{\mathrm{T}}^{\mathrm{miss}} \geq 50$ GeV from $\gamma\gamma$, ff, and $Z \to ee$ as well as the combined background.

Type	Events	stat. error	syst. error
$\gamma\gamma$ candidates	9		
Total background (ff)	12.7	± 5.0	
Total background (ee)	11.1	± 2.1	
Combined background	11.3	± 1.9	± 0.8

certainty (4-66%) and renormalization scale (4-28%) uncertainty depending on the SUSY signal masses.

We estimate a total $E_{\mathrm{T}}^{\mathrm{miss}} \geq 100$ GeV background of $1.5 \pm 0.8\,(\mathrm{stat.}) \pm 0.6\,(\mathrm{syst.})$ events from the error weighted combination of the two ways of determining QCD backgrounds, plus the EWK background. Using this measurement and the acceptance times efficiency for the SUSY GGM MC and employing a $\mathrm{CL_S}$ limit-setting method [27], we determine upper limits for GGM SUSY production. We test Gaussian, log-normal and gamma shapes as different models to incorporate uncertainties on the total background rate, integrated luminosity, and total acceptance times efficiency. The observed 95% CL cross-section limits vary between 0.015 and 0.03 pb depending on SUSY masses, and are shown in Fig. 2 for squark and gluino masses between 400 and 2000 GeV/c^2 and a neutralino mass of 375 GeV/c^2.

The single-photon analysis is based on a trigger requiring the presence of one photon with $E_{\mathrm{T}} > 70$ *GeV* and the scalar sum of the energies of all objects in the event (H_{T}) to be greater than 350 GeV. The offline analysis requires $H_{\mathrm{T}} \geq 400$ GeV for the H_{T} trigger to become fully efficient, and requires exactly one photon with $E_{\mathrm{T}} > 75$ GeV within $|\eta| < 1.4$. In addition, we require ≥ 3 jets with $p_{\mathrm{T}} \geq 30\,\mathrm{GeV}/c$ and $|\eta| \leq 2.6$.

The photon/QCD background in the single-photon analysis is a composition of direct photon-jet production and of QCD multijet production, where one jet is misidentified as a photon. The shape of the MET distribution, including the non-Gaussian tails, is similar for both background contributions, as the event topology is very similar between the two. Therefore, these two QCD contributions are estimated together from the same data control sample. The control sample is selected by applying the same signal selection requirements, except that the photon candidate is required to fail the tight selection criteria but satisfy a loose isolation requirement. We refer to such photon candidates as γ_{jet}, whose identification is by definition orthogonal to

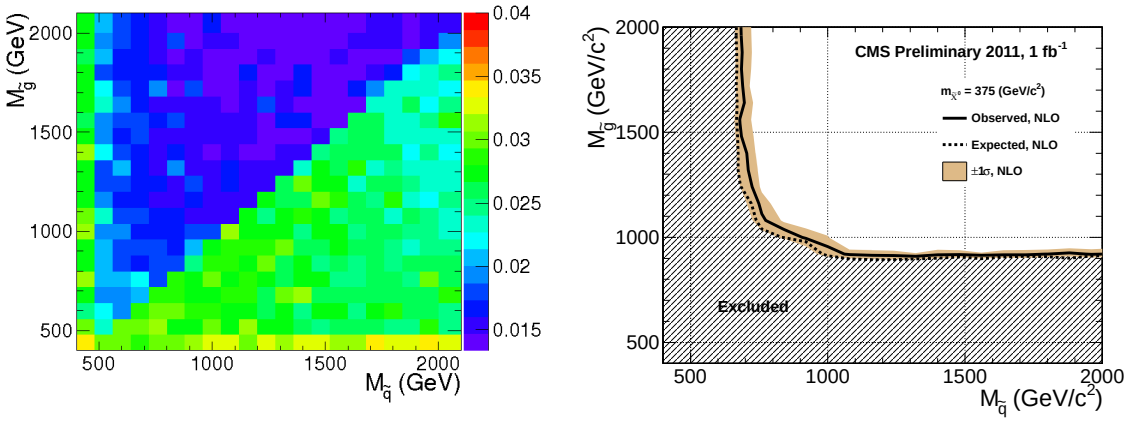

Figure 2: 95% CL upper limits on the cross section (left) and exclusion contours (right) in gluino-squark mass space for a neutralino mass of $m(\tilde{\chi}_1^0) = 375$ GeV/c^2. The shaded uncertainty band around the exclusion contour corresponds to the NLO renormalization and PDF uncertainties of the signal cross section.

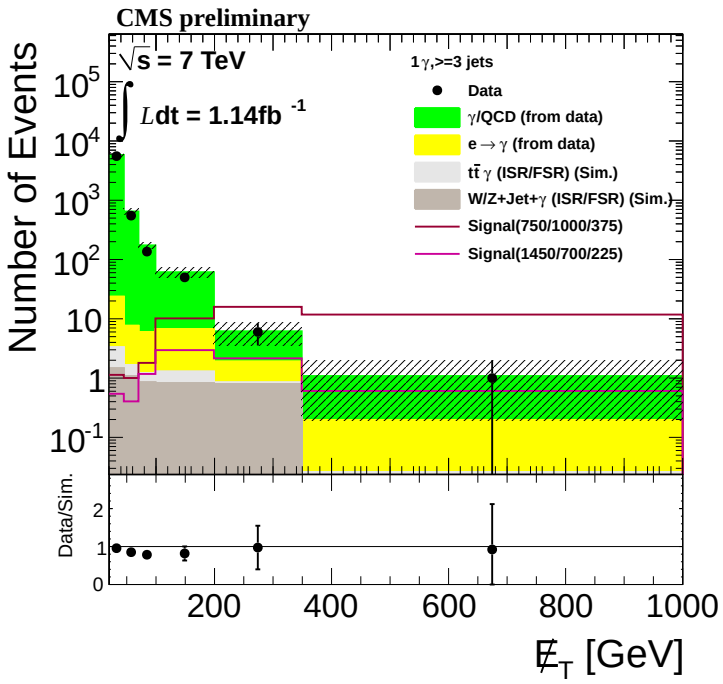

Figure 3: Total standard model background prediction compared to the number of single-photon events, including two GGM benchmark signal benchmark points as examples where masses ($m_{\tilde{q}}/m_{\tilde{g}}/m_{\tilde{\chi}^0_1}$) are given in GeV/$c^2$.

the photon ID criteria in the signal selection. The control sample has to be weighted, to correct for the different p_T spectra of γ_{jet} and tight photon objects in the control and signal samples, respectively. The weights are determined in a signal-depleted region with $E_T^{miss} < 100$ GeV and the weight vs. photon candidate E_T is found to be reasonably described by a Landau function.

The strategy to model the electroweak background contribution, which is much smaller than the QCD background, is similar to that in the diphoton analysis, as described above. The dominant contributions are from $t\bar{t}$ production or events with W or Z bosons with one or more neutrinos in the final state. Additional backgrounds can occur due to initial state radiation (ISR) and final state radiation (FSR) of photons. ISR and FSR in events with electrons in the final state are already covered by the electroweak background prediction from data and the remaining contributions from SM process are very small and directly taken from Monte Carlo simulation with a systematic uncertainty of 100%. These remaining backgrounds are summarized in Table 4.

A study of sensitivity versus E_T^{miss} requirement suggests a value of 200 GeV to be inclusive for the different GGM signals and also obtain stringent limits. The combined background prediction, the observed data and two GGM benchmark signal samples, one excluded and one included, are shown in Fig. 3. For $E_T^{miss} > 200$ GeV, seven events are observed in 1.14 fb^{-1} of data, while a total of $7.24 \pm 2.6\,(\text{stat.}) \pm 1.5\,(\text{syst.})$ backgrounds events are expected from SM sources. The expected and observed event yields are summarized in Table 4. No excess beyond standard model predictions is observed.

In the same way as described for the diphoton analysis above, we use the CL_S method to determine 95% confidence level upper limits for the squark versus gluino mass plane from 400 GeV/c^2 to 2000 GeV/c^2 in squark mass and 400 GeV/c^2 to 1300 GeV/c^2 in gluino mass with

Table 4: Resulting event yields for the $\gamma + 3$ jets $+ E_{\mathrm{T}}^{\mathrm{miss}}$ selection for $E_{\mathrm{T}}^{\mathrm{miss}} > 200$ GeV.

Sample	Event yield		
		(stat.)	(syst.)
Data	7		
QCD (est. from data)	5.16	$\pm$2.58	$\pm$0.62
EWK $e \to \gamma$ (est. from data)	1.22	$\pm$0.13	$\pm$0.04
FSR/ISR ($W \to \mu/\tau\nu, \mathrm{Z} \to \nu\nu$) (Sim.)	0.80	$\pm$0.31	$\pm$0.80
FSR/ISR ($\mathrm{t\bar{t}} \to \mu/\tau\nu + X$) (Sim.)	0.07	$\pm$0.05	$\pm$0.07
Total SM background estimate	7.24	$\pm$2.6	$\pm$1.53

neutralino mass set at 375 GeV/c^2. We have studied two different models for the neutralino mixture. One where the neutralino is bino-like and decays into a gravitino and a photon or a Z boson and a scenario where the neutralino is a pure wino. In this case the lightest chargino is also wino-like and the chargino-neutralino mass difference is too small for one to decay into the other. Therefore the chargino will decay directly into a gravitino and a W boson. In that case we expect much less photon production and the acceptance will drop for the single-photon selection.

A possible contamination of signal in the background sample used for the background estimation has been studied and is considered in the limit calculation. The expected amount of SUSY GGM events in the background estimation has been subtracted from the number of observed signal events, lowering the acceptance times efficiency by a few percent for each point. The resulting limits, after subtraction of the signal contamination, are shown in Fig. 4. For the bino-like scenario the resulting upper limit cross section is of order 0.05 pb with a typical acceptance of $\sim$ 25%. For the wino like scenario the acceptance drops to $\sim$ 5%, leading to an upper limit cross section of $\sim$ 0.2 pb.

In summary, we have searched for evidence of GGM SUSY production in diphoton and single-photon events using the $E_{\mathrm{T}}^{\mathrm{miss}}$ spectrum beyond 100 GeV and 200 GeV, respectively. This search is based on 2011 CMS data comprising 1.14 fb^{-1} of pp collisions at $\sqrt{s} = 7$ TeV. We find no evidence of GGM SUSY production and set upper limits for a range of parameters in that model. In the diphoton analysis we have defined exclusion regions in the GGM SUSY parameter space of squark, gluino and neutralino masses at the level of 0.015 to 0.03 pb for the respective production cross section. For the single-photon analysis the resulting 95% CL upper limit cross section for a similar scan in GGM SUSY parameter space is of order 0.05 pb (0.2 pb) for the bino- (wino-) like scenarios.

References

[1] P. Fayet, "Mixing Between Gravitational and Weak Interactions Through the Massive Gravitino", *Phys. Lett.* **B70** (1977) 461. doi:10.1016/0370-2693(77)90414-2.

[2] H. Baer, M. Brhlik, C. H. Chen et al., "Signals for the Minimal Gauge-Mediated Supersymmetry Breaking Model at the Fermilab Tevatron Collider", *Phys. Rev.* **D55** (1997) 4463. doi:10.1103/PhysRevD.55.4463.

[3] H. Baer, P. G. Mercadante, X. Tata et al., "Reach of Tevatron Upgrades in Gauge-Mediated Supersymmetry Breaking Models", *Phys. Rev.* **D60** (1999) 055001. doi:10.1103/PhysRevD.60.055001.

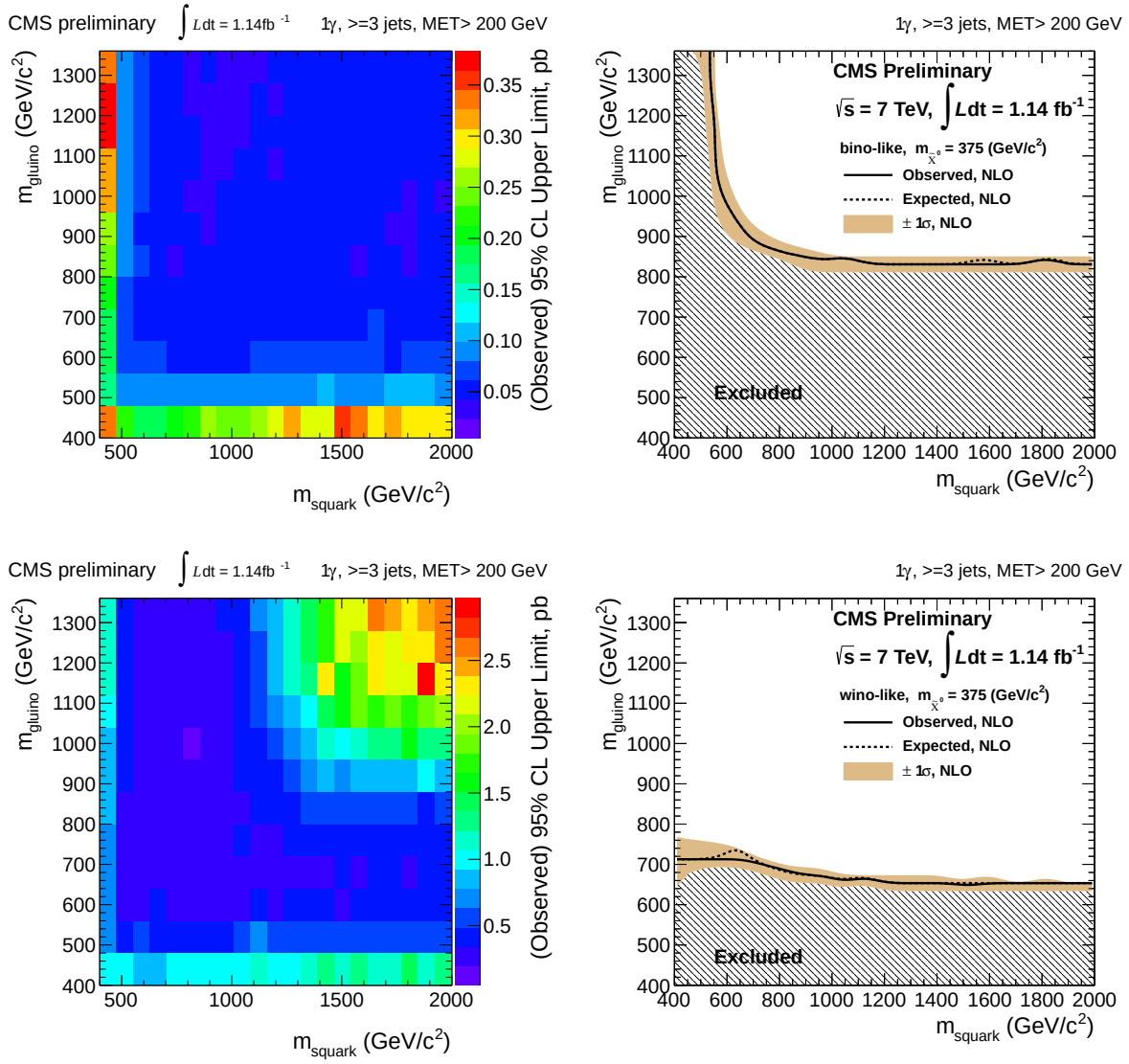

Figure 4: 95% CL upper limits (left) and exclusion contours (right) for bino (top) and wino (bottom) like neutralino. The shaded uncertainty band around the exclusion contours correspond to the NLO renormalization and PDF uncertainties of the signal cross section.

[4] S. Dimopoulos, S. Thomas, and J. D. Wells, "Sparticle Spectroscopy and Electroweak Symmetry Breaking with Gauge-Mediated Supersymmetry Breaking", *Nucl. Phys.* **B488** (1997) 39. doi:10.1016/S0550-3213(97)00030-8.

[5] J. R. Ellis, J. L. Lopez, and D. V. Nanopoulos, "Analysis of LEP Constraints on Supersymmetric Models with a Light Gravitino", *Phys. Lett.* **B394** (1997) 354. doi:10.1016/S0370-2693(97)00019-1.

[6] M. Dine, A. Nelson, Y. Nir et al., "New Tools for Low Energy Dynamical Supersymmetry Breaking", *Phys. Rev.* **D53** (1996) 2658. doi:10.1103/PhysRevD.53.2658.

[7] G. F. Giudice and R. Rattazzi, "Gauge-Mediated Supersymmetry Breaking", in *Perspectives on Supersymmetry*, p. 355. World Scientific, Singapore, 1998.

[8] ATLAS Collaboration Collaboration, "Search for Diphoton Events with Large Missing Transverse Energy with 30 $pb^{-}1$ of 7 TeV Proton-Proton Collision Data with the ATLAS Detector", arXiv:1107.0561. * Temporary entry *.

[9] CMS Collaboration, "Search for Supersymmetry in pp Collisions at sqrt(s) = 7 TeV in Events with Two Photons and Missing Transverse Energy", *Phys. Rev. Lett.* **106** (2011) 211802. doi:10.1103/PhysRevLett.106.211802.

[10] T. Aaltonen et al., "Search for Supersymmetry with Gauge-Mediated Breaking in Diphoton Events with Missing Transverse Energy at CDF II", *Phys. Rev. Lett.* **104** (2010) 011801. doi:10.1103/PhysRevLett.104.011801.

[11] V. M. Abazov et al., "Search for Diphoton Events with Large Missing Transverse Energy in 6.3 fb^{-1} of $p\bar{p}$ Collisions at $\sqrt{s}$ = 1.96 TeV", *Phys. Rev. Lett.* **105** (2010) 221802. doi:10.1103/PhysRevLett.105.221802.

[12] A. Heister et al., "Search for Gauge Mediated SUSY Breaking Topologies in e^+e^- Collisions at Centre-of-Mass Energies up to 209 GeV", *Eur. Phys. J.* **C25** (2002) 339. doi:10.1007/s10052-002-1005-z.

[13] J. Abdallah et al., "Photon Events with Missing Energy in e^+e^- Collisions at $\sqrt{(}s) = 130$ to 209 GeV", *Eur. Phys. J.* **C38** (2005) 395. doi:10.1140/epjc/s2004-02051-8.

[14] P. Achard et al., "Single- and Multi-Photon Events with Missing Energy in e^+e^- Collisions at LEP", *Phys. Lett.* **B587** (2004) 16. doi:10.1016/j.physletb.2004.01.010.

[15] G. Abbiendi et al., "Search for Gauge-Mediated Supersymmetry Breaking Topologies in e^+e^- Collisions at LEP2", *Eur. Phys. J.* **C46** (2006) 307. doi:10.1140/epjc/s2006-02524-8.

[16] A. Aktas et al., "Search for Light Gravitinos in Events with Photons and Missing Transverse Momentum at HERA", *Phys. Lett.* **B616** (2005) 31. doi:10.1016/j.physletb.2005.04.038.

[17] LHC New Physics Working Group, "Simplified Models for LHC New Physics Searches", (2010). See http://www.lhcnewphysics.org/photons.

[18] P. Meade, N. Seiberg, and D. Shih, "General Gauge Mediation", *Prog. Theor. Phys. Suppl.* **177** (2009) 143. doi:10.1143/PTPS.177.143.

[19] M. Buican, P. Meade, N. Seiberg et al., "Exploring General Gauge Mediation", *JHEP* **0903** (2009) 016. doi:10.1088/1126-6708/2009/03/016.

[20] G. R. Farrar and P. Fayet, "Phenomenology of the Production, Decay, and Detection of New Hadronic States Associated with Supersymmetry", *Phys. Lett.* **B76** (1978) 575. doi:10.1016/0370-2693(78)90858-4.

[21] CMS Collaboration, "The CMS experiment at the CERN LHC", *JINST* **03** (2008) S08004. doi:10.1088/1748-0221/3/08/S08004.

[22] P. Adzic et al., "Energy resolution of the barrel of the CMS electromagnetic calorimeter", *JINST* **2** (2007) P04004. doi:10.1088/1748-0221/2/04/P04004.

[23] CMS Collaboration, "Particle–Flow Event Reconstruction in CMS and Performance for Jets, Taus, and $E_{\mathrm{T}}^{\mathrm{miss}}$", *CMS Physics Analysis Summary* **CMS-PAS-PFT-09-001** (2009).

[24] T. Sjostrand, S. Mrenna, and P. Z. Skands, "PYTHIA 6.4 Physics and Manual", *JHEP* **0605** (2006) 026, arXiv:hep-ph/0603175. doi:10.1088/1126-6708/2006/05/026.

[25] W. Beenakker, R. Höpker, M. Spira et al., "Squark and Gluino Production at Hadron Colliders", *Nucl. Phys.* **B492** (1997) 51. doi:10.1016/S0550-3213(97)80084-9.

[26] GEANT4 Collaboration, "GEANT4: A Simulation toolkit", *Nucl.Instrum.Meth.* **A506** (2003) 250–303. doi:10.1016/S0168-9002(03)01368-8.

[27] Particle Data Group Collaboration, "Review of particle physics", *J. Phys.* **G37** (2010) 075021. doi:10.1088/0954-3899/37/7A/075021.